Prediction of bubble size distribution in mechanical flotation cells

by F. Sawyerr, D.A. Deglon, and C.T. O'Connor*

Synopsis

A bubble population balance model is proposed for the prediction of Sauter mean bubble diameters in mechanical flotation cells. In the model, the flotation cell is treated as two separate, statistically homogeneous zones—the impeller zone, and the bulk tank zone. Balance functions for the rates of bubble breakage, coalescence, recirculation and inlet-outlet events are proposed based on classical chemical engineering research in two- and three-phase fluid mixing systems. An initial simulation of the population balance model shows trends in bubble size distributions comparable to measured distributions in industrial mechanical flotation cells.

Introduction

Froth flotation is a complex physico-chemical process used widely in the minerals processing industry to separate valuable minerals from gangue in low-grade ores. In flotation, air bubbles are introduced into a vessel containing a slurry of the ore, and hydrophobic particles in the slurry attach themselves to air bubbles and are transported out of the vessel by the buoyant rise of the bubbles. The process as a whole depends on the control of the pulp chemistry to enhance the hydrophobicity of the valuable minerals and reduce the floatability of the gangue material, and also on the gas dispersion and hydrodynamics in the flotation cell, which control the contacting between particles and bubbles. While extensive research has been carried out on manipulation of pulp chemistry to optimize recovery of specific minerals, detailed studies on the physical mechanism of flotation have only recently begun to appear in the flotation literature. This intensification in research efforts to better understand gas dispersion and hydrodynamics in flotation cells has come about because of the growing need to design larger and more efficient flotation cells to treat the lower grade and more finely disseminated ores that are currently being mined.

Studies on the effects of the gas phase have shown that in flotation, like in other gas-liquid mass transfer processes, the rate of mineral recovery is intimately linked to the bubble size distribution in the flotation vessel. Ahmed and Jameson[1] reported an almost one-hundred-fold increase in the rate of fine quartz flotation when the average bubble size in their batch flotation cell was reduced from 655 to 75 μm, and Yoon and Luttrell[26] showed theoretically that the probability of contact between particles and bubbles in flotation varies as the inverse of the bubble size raised to a power of between 1 and 2. More recently, Gorain[10] and co-workers in the AMIRA P9 project observed a linear relationship between the first order flotation rate constant and the bubble surface area flux in a mechanical flotation cell. They concluded that the bubble surface area flux, which is proportional to the superficial gas velocity and inversely proportional to the Sauter mean bubble diameter, can be used as a single, scaleable parameter to characterize the physical contribution of the flotation cell to the rate of mineral recovery. All of these studies clearly show that knowledge of the bubble size distribution is essential to the prediction of the cell's metallurgical performance.

Thus far, bubble size distributions in flotation cells have been determined through direct measurement using primarily the capillary tube technique (Jameson and Allum[12], Tucker[23] *et al.*), and also by photographic means. However, for the prediction of the performance of a hypothetical flotation cell from design specifications, or for the simulation of an entire flotation circuit, a model is required to predict the bubble size distribution from basic operating parameters. The drift flux analysis technique (Yianatos[25] *et al.*), has been successfully used to predict the mean bubble size in flotation columns, but no tenable model has yet been proposed for the prediction of bubble size in mechanically

* *Minerals Processing Research Unit, Department of Chemical Engineering, University of Cape Town, Rondebosch, 7700*

 SA ISSN 0038–223X/3.00 + 0.00. Paper received May 1998; revised paper received Jun. 1998.

agitated flotation cells. The objective of this study is to derive a model for the prediction of bubble size distribution in mechanical flotation cells by investigating the fundamental gas dispersion mechanisms occurring in the mechanical flotation cell. It is hoped that this approach will lead not only to a practically useful bubble size predictor, but also to a deeper understanding of the microprocesses taking place in the flotation cell which will enable design of more efficient flotation cells. In this paper, a review of literature on the prediction of Sauter mean bubble diameters will be presented, followed by a description of the methodology to be employed to predict Sauter mean bubble diameters, and finally some preliminary results will be shown.

Literature review

The traditional approach to modelling gas dispersion in mechanical flotation cells has generally not involved micro-properties such as bubble size distribution, but has rather dealt with macroscopic properties of the system. Bulk dimensionless parameters such as the air flow number, the power number and the Froude number have typically been used to characterize the hydrodynamics of flotation cells, and empirical relationships between groups of these parameters formed the basis for design and scale-up of flotation cells (Arbiter[2] *et al.*). This approach gives little scope for prediction of bubble size as it only involves a macroscopic overview of the process and does not take into account the basic gas-phase sub-processes occurring in the flotation cell. In fact, to the authors' knowledge, despite the availability of accurate bubble size measurements in flotation literature for over 10 years (Jameson and Allum[12]) no tenable model to predict bubble size in terms of bulk dimensionless parameters has yet been proposed. A more fundamental analysis of the micro-processes of gas dispersion is required in order to predict bubble size distribution.

Fundamental studies of this nature are not available in the flotation literature and insight into modelling bubble size distributions has been gained from classical chemical engineering research in two- and three-phase fluid mixing systems and bioreactor design. These studies have generally been carried out in standard baffled tanks agitated by a six-bladed Rushton turbine and though these test conditions are not *per se* identical to those in industrial flotation cells, the underlying mechanisms of gas dispersion occurring in them are essentially the same. Theory from these studies is thus a good starting point for modelling gas dispersion in mechanical flotation cells.

The basic mechanism of gas dispersion under highly turbulent conditions has been written about by a number of researchers. In mechanically agitated, aerated vessels, such as flotation cells, air introduced into the cell accumulates in low pressure cavities behind the impeller blades and bubbles are sheared off the cavities by the impeller's rotation (Tatterson[21]). These bubbles are further broken under the turbulent conditions in the impeller region and are then dispersed throughout the cell by the pumping action of the impeller. In the bulk region of the cell, bubble motion is controlled by the surrounding fluid circulatory motion and by the bubble's inherent buoyancy. Bubbles in this region may collide and coalesce, recirculate back to the impeller region, or rise out of the cell. The equilibrium bubble size distribution in the cell is ultimately dictated by all the events taking place in the cell, in particular by the relative rates of bubble breakage and bubble coalescence in the cell.

Because in practice it is difficult to determine, independently, the rates of breakage and coalescence in a dynamic system, most reported studies have dealt with systems in which either one or the other phenomenon was suppressed such that the other could be studied. In studies carried out in systems with high surfactant concentration, where coalescence was negligible, researchers have shown that mean bubble size can be effectively modelled using Hinze's bubble breakage model.

Hinze's model of turbulent pressure fluctuations, which is the most widely accepted model for bubble breakage, describes a bubble in a turbulent flow field as experiencing dynamic pressure forces which tend to deform it, and surface tension forces which tend to resist the deformation. When the ratio of these two forces, defined as the Weber number (N_{We}), exceeds a critical value the bubble is broken up. As the diameter of a bubble decreases, the deforming force decreases and the restoring stress increases until eventually a critical diameter, called the maximum stable bubble size (d_{max}), is reached where the deforming stress is unable to break the bubble. Using this theory Chen and Middleman[6] proposed the following expression for d_{max}:

$$\frac{d_{max}}{D} = C_1 N_{We}^{\pm 0.6} \qquad [1]$$

Experimental data shows a strong relationship between d_{max} and the Sauter mean bubble diameter (d_s) and several researchers have expressed d_s as the product of Hinze's d_{max} and an empirically determined constant, for high surfactant, non-coalescing systems. Calabrese[3] *et al.* correlated experimental data for low dispersed phase viscosity with the following expression:

$$\frac{d_s}{D} = 0.053 N_{We}^{\pm 0.6} \qquad [2]$$

Calderbank[4] proposed this expression based on Kolmogoroff's[14] theory of isotropic turbulence:

$$d_s = C \frac{\sigma^{0.6}}{(P/V_i)^{0.4} \rho^{0.2}} \varepsilon^n \left(\frac{\mu_G}{\mu_L} \right)^{0.25} \qquad [3]$$

And Parthasarathy[19] *et al.* fitted this model to experimental bubble size data and obtained:

$$d_s = \frac{2.0\left(\sigma^{0.6}\right)}{\left(P/V_i\right)^{0.4}\left(\rho\right)^{0.2}} \qquad [4]$$

Lu[17] *et al.* also published a semi-empirical correlation for Sauter mean diameter in a non-coalescing environment in terms of the specific power input and the air flow rate.

Semi-empirical correlations based on Hinze's[11] bubble breakage theory give a reasonably good approximation of the fundamental bubble breakage events occurring in the cell and can accurately predict the bubble size distribution in the impeller discharge region of the cell. These correlations, however, are inadequate for prediction of real industrial

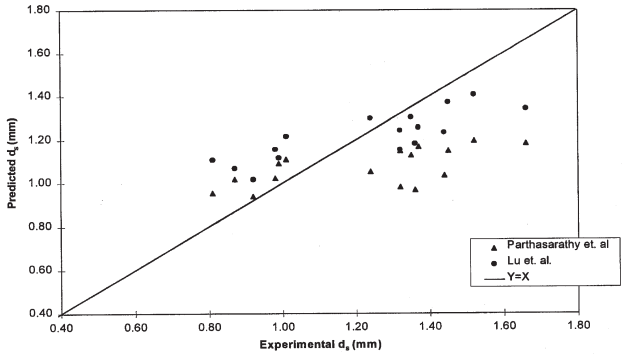

Figure 1—Comparison between Gorain's experimental Sauter mean diameters and model predictions of Parthasarathy *et al* and Lu *et al*

conditions, because they do not take into account important events happening in the bulk of the cell—such as bubble recirculation and bubble coalescence—that also influence d_s. Figure 1 shows a comparison between experimental Sauter mean diameters from Gorain's[10] *et al.* k-S_b testwork and values predicted by Parthasarathy[19] *et al.* and Lu[17] *et al.* Though the predicted values are of the same order as the experimental data, and lend credence to the predictive powers of the bubble breakup model, there is considerable scatter about line y = x, particularly at higher bubble diameters, due to the effects of coalescence.

Published industrial bubble size measurements show that in most instances d_s in the upper region of the flotation cell is larger than d_s in the impeller discharge region, indicating that despite the fairly high frother concentrations used in flotation, bubble coalescence does in fact take place. Clearly, the rate of bubble coalescence must be taken into account in the prediction of d_s.

Investigations into bubble coalescence reported in the literature have isolated the coalescence rate by eliminating the contribution of bubble breakage to the equilibrium bubble size distribution. This has been done either by employing very quiescent bubble columns where the rate of bubble breakage was negligible, or by sparging bubbles into the system that were too small to be broken up by the impeller. Results from the former type of study are not applicable to mechanical flotation cells, and it is from the latter studies that our current understanding of the mechanism of bubble coalescence is derived.

Nagaraj and Gray[18], measured gas-liquid interfacial areas in an air-sparged cell agitated with a Rushton turbine for a range of particle sizes and slurry densities and found that the coalescence rate increased with increasing solids concentration. They postulated that the presence of solids reduces the turbulent intensity in the cell, which reduces the bubble approach velocity and thereby lengthens the average bubble contact time, enhancing coalescence. Prince and Blanch[20] modelled the coalescence frequency as the product of the bubble collision frequency and the attachment efficiency. They expressed the collision frequency (θ_{ij}) in terms of the hydrodynamics in the cell, and for highly turbulent systems used the relationship:

$$\theta_{ij} = 0.089\pi n_i n_j \left(d_i + d_j\right)^2 \varepsilon^{1/3} \left(d_i^{2/3} + d_j^{2/3}\right)^{1/2} \qquad [5]$$

The attachment efficiency (λ) was expressed as a function of the contact time between bubbles (τ_{ij}) and the time required for bubbles to coalesce (t_{ij}):

$$\lambda_{ij} = \exp\left(-t_{ij} / \tau_{ij}\right) \qquad [6]$$

Here, coalescence time is assumed to be the time taken for the film separating two bubbles to thin and rupture. Fluid surface tension and the initial film thickness, both of which are functions of the frother concentration in the fluid, govern the rate of this phenomenon. The bubble contact time is dependent on the bubble size and the turbulent intensity and was derived by Levich[16] as:

$$\tau_{ij} = \frac{r_b^{2/3}}{\varepsilon^{1/3}} \qquad [7]$$

Despite the presence of a bubble size term in the above expression, Prince and Blanch[20] found that the coalescence frequency was virtually independent of bubble size. They explain this by pointing out that though large bubbles have higher velocities and larger collisional cross-sectional areas, which lead to higher collision frequencies, they also have larger coalescence times and lower attachment efficiencies which offset the higher collision frequencies.

It is evident that both coalescence and breakage are complex, interdependent phenomena that are influenced by the instantaneous state of the system. In systems such as the mechanical flotation cell, where both bubble breakup and coalescence are taking place, a single correlation is not sufficient to accurately predict d_s. The most effective methodology for prediction of bubble size distribution in such systems is the population balance equation. This model describes the history of a bubble population in terms of numbers and volumes of bubbles as the bubbles interact with themselves and the surrounding environment. The model can at the same time accommodate bubble breakage, coalescence and inlet-outlet phenomena and provides a dynamic simulation of the effects of operating parameters on the equilibrium size of the distribution. The population balance model has been used successfully by Lee[15] *et al.* and Prince and Blanch[20] to model bubble size distributions in bubble column reactors and has also been successfully used by others to model drop size distributions in mechanically mixed, liquid-liquid dispersions (Chatzi and Kiparissides[5], Coulalouglou and Tavlarides[7]). In the following section details of a bubble population balance for prediction of Sauter mean bubble diameters in a mechanical flotation cell will be presented.

Population balance model

In classical formulations of the bubble population balance (e.g. Prince and Blanch[20]) the system under investigation was assumed to be well mixed, and bubble size distribution was taken to be uniform throughout the system. Thus a single balance could be performed over the whole system, neglecting the effect of variations in spatial distribution, and simultaneously incorporating the effects of bubble breakage and coalescence. In the mechanical flotation cell, we know from industrial data that there is significant variation in the bubble size distribution between the impeller region and the bulk of the tank, and it would be inaccurate to perform a

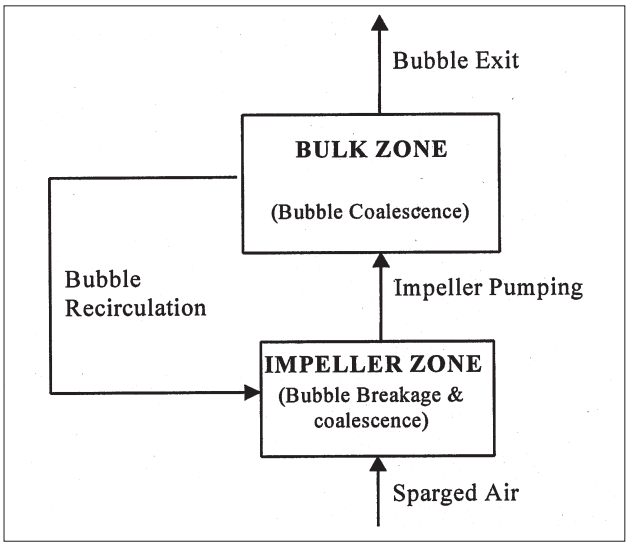

Figure 2—Schematic of the bubble population balance zones in a mechanical flotation cell

population balance over the whole cell assuming statistical homogeneity of bubble size. As such, in this study, the mechanical flotation cell will be modelled as two separate systems—the impeller zone, which includes the impeller swept volume and the impeller discharge stream, and the bulk zone, as shown in Figure 2. Within each zone the distribution of bubbles is assumed to be statistically homogeneous, an assumption that is validated by industrial bubble size data (Egya-Mensah[8]). Bubble breakage is assumed to happen only in the impeller zone because of the much higher rate of energy dissipation in this zone relative to the bulk zone (Wu and Patterson[24]), while bubble coalescence is assumed to take place in both zones. Freshly sparged gas enters the impeller zone, together with recirculated gas from the bulk zone, and bubbles from the impeller zone are transported to the bulk zone by the pumping action of the impeller. From the bulk zone, bubbles are either recirculated back into the impeller zone or exit the cell by rising into the froth phase.

The population balance is solved by performing a bubble number balance around each of the zones.

Impeller zone

If we let $N^I(v, t)$ represent the number of bubbles of volume v in the impeller zone per unit volume at time t, then the bubble population balance in the impeller zone can be written as follows:

$$\frac{\partial}{\partial t}\left[N^I(v,t)\right] = \int_v^{v_{max}} B(v')N_d D(v',v)N^I(v',t)dv' - B(v)N^I(v,t) + n_0(v,t) + R(v)Q_I N^B(v,t) - Q_I N^I(v,t) \quad [8]$$

The first two terms on the right-hand side represent the rate of formation and loss of bubbles of volume v respectively due to breakage. Here, $B(v)$ is the breakage frequency, N_d is the number of daughter bubbles formed, and $D(v',v)$ is the distribution of daughter fragments formed from breakage of bubble if size v'. The next two terms describe the flow of bubbles into the impeller region by sparging and recirculation

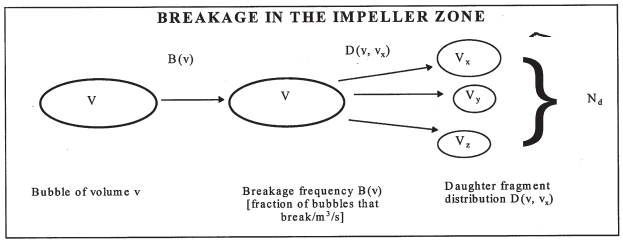

Figure 3—Breakage in the impeller zone

respectively. Here $n_0(v, t)$ is the number of new bubbles sparged with volume v. $R(v)$ is the recycle frequency of bubbles of volume v, $N^B(v, t)$ is the number of bubbles of volume v in the bulk zone, and Q_I is the volumetric pumping rate of the impeller. The last term accounts for the rate at which bubbles exit the impeller zone by the pumping action of the impeller.

Bulk zone

If we assume that the rate of bubble coalescence in the bulk zone is independent of bubble volume (Prince and Blanch[20]), we can define an overall coalescence frequency, K, that is determined by the hydrodynamic conditions in the bulk zone. The frequency of coalescence of bubbles of volume v and v' will then be proportional to the product of the number fractions of bubbles of size v and v'. The population balance in the bulk zone can be expressed as follows:

$$\frac{\partial}{\partial t}\left[N^B(v,t)\right] = Q_I N^I(v,t) - KN^B(v,t)\int_{v_{min}}^{v_{max}}\left[\frac{N^B(v',t)}{N^{B(T)}}\right]dv' + KN^B(T)C(v) - R(v)Q_I N^B(v,t) - N^B(v,t)U(v)A_b \quad [9]$$

Here, the first term on the right hand side is the number of bubbles of volume v pumped over from impeller region and the next two terms represent the loss and formation of bubbles of volume v through coalescence respectively. $N^B(T)$ is the total number of bubbles in the bulk zone and the ratio $[N^B(v',t) / N^B(T)]$ is the number fraction of bubbles with volume v. $C(v)$ is the fraction of all coalescence events that form a new bubble of volume v. The last two terms concern the loss of bubbles from the bulk zone through recirculation and bubble exit respectively. $U(v)$ is the rise velocity of bubble with volume v, and A_b is the cross-sectional area of the bulk zone.

Population balance functions

Breakage frequency, B (v)

In the bubble breakage models of Prince and Blanch[20] and Tsouris and Tavlarides[22] bubble breakage is assumed to occur

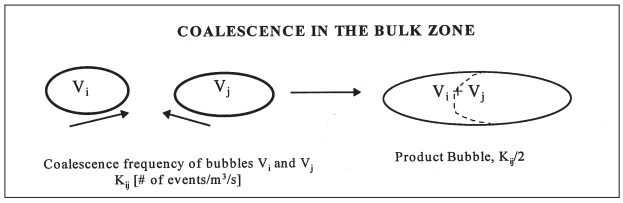

Figure 4—Coalescence in the bulk zone

through collisions between bubbles and turbulent eddies of length scale smaller than the bubble diameter. The breakage frequency is defined as the product of the bubble-eddy collision frequency and the breakage efficiency. Though the formulation of the expression requires knowledge of the spectral energy density of the eddies in the inertial subrange, and is therefore inappropriate for use in the modelling of an industrial floatation cell, the model highlights several important factors in the breakage rate. Firstly, bubble breakage frequency goes down with decreasing bubble size and drops to zero at the maximum stable bubble size (d_{max}), and secondly, the breakage frequency reduces with increasing gas holdup (ϕ). On this basis the following general functional form for the breakage frequency is proposed.

$$B(v) = C_1 f(\phi)\left[\exp(C_2 d) - \exp(C_2 d_{\max})\right] \quad [10]$$

The function $f(\phi)$ tends to zero as the holdup increases to 1, and the breakage frequency decreases exponentially as the bubble diameter tends to d_{max}.

Daughter fragment distribution, D(v',v)

The number of daughter fragments formed from the breakage of a single bubble, N_d will remain a variable parameter in the population balance. After the work of Chatzi and Kiparissides[5] it will be assumed that the daughter fragment volumes formed from the breakage of a bubble will be normally distributed about the mean daughter fragment volume, with a standard deviation (σ_v) equal to one-third the mean daughter fragment volume. Thus:

$$D(v', v) = \frac{1}{\left[\sigma_v \sqrt{2\pi}\right]} \exp\left[\frac{-(v - v_{mean})^2}{2\sigma_v{}^2}\right] \quad [11]$$

Coalescence frequency, K

The coalescence frequency is assumed to be independent of bubble size (Prince and Blanch[20]) and is modelled as a global parameter determined by the hydrodynamic conditions in the cell. Combining equations [6] and [7], and substituting specific power, P/V for rate of energy dissipation (ε), the following expression for the coalescence frequency is proposed:

$$K = C_1 (P/V)^{1/3} \exp\left[-C_2 (P/V)^{1/3}\right] \quad [12]$$

The constant C_2 represents the coalescence, or film-thinning, time and is a function of frother concentration. The number of coalescence events, $N_c(v_i, v_j)$, between bubbles of volumes v_i and v_j is expressed in terms of the probability of these bubbles colliding, and is given by the product of their respective number fractions (c_i, c_j) multiplied by the overall coalescence rate. Thus:

$$N_c(v_i v_j) = K N_b(T) c_i c_j \quad [13]$$

Gas recirculation, R (v)

The overall rate of gas recirculation from the bulk zone to the impeller zone of a flotation cell can be calculated from the bubble number fraction and the impeller pumping rate. It is assumed that the fluid flow rate from the bulk zone to the impeller zone is equal to the impeller pumping rate and that the probability of a bubble recirculating from the bulk to the impeller region, $R(v)$, is a function of the bubble size. Though there is no available literature on the influence of bubble size on recirculation frequency, it is known that smaller bubbles are more likely to be recirculated as they have lower rise velocities. As such a relationship is proposed for $R(v)$ based on the bubble rise velocity:

$$R(v) = \frac{C_1}{U(v)} \quad [14]$$

Bubble rise velocity, U(v)

Bubble rise velocity is estimated using Karamanev's[13] correlation for the terminal rise velocity of air bubbles in water containing a high concentration of surfactant. The expression is:

$$U(v) = 37.1 d^{1/2} \quad [15]$$

Dynamic population balance simulation

As an analytical solution of the population balance equation is not possible, a numerical technique is required. This is done by transforming the population balance equation into a system of differential equations by discretizing the range of bubble volumes. In this study the volume range of bubbles was divided into 20 classes geometrically spaced from 0.2 mm to 5 mm, typical of the range of bubble sizes observed in industrial flotation cells. Initial values for the constants in the various balance functions are assumed, and a dynamic simulation of the drop population with a variable time step is run using Microsoft Excel. A least squares solver technique is used to fit the simulation results to actual industrial data so that the constants in the various functions can be approximated. Figure 5 shows an example of some typical results of a dynamic bubble population balance in a hypothetical flotation cell using the physical parameters of the 2.8 m^3 flotation cell employed by Gorain[10] *et al.*, in the original k-S_b testwork.

In Figure 5, which depicts the bubble size distribution in the bulk zone of the hypothetical flotation cell calculated from bubble volumes, it can be seen that the distribution

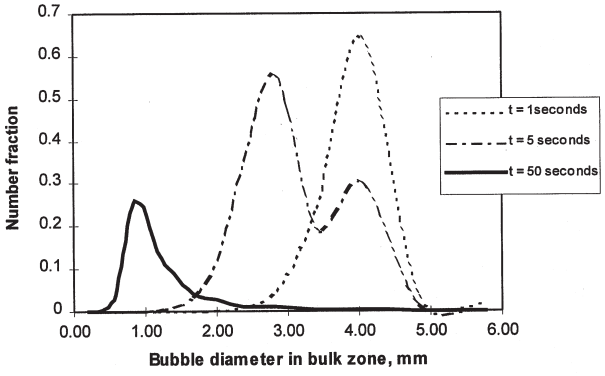

Figure 5—Sample results of a dynamic bubble population balance simulation

moves from a normal distribution about a large bubble size (an input to the simulation) through a bimodal distribution, to a log-normal steady-state distribution. These trends mimic those observed from industrial bubble size data and provide encouragement that the population balance can be used to successfully predict Sauter mean bubble size in industrial flotation cells.

Future work

The population balance model presented in this paper represents the fundamental framework for prediction of bubble size distribution in flotation cells. The various functional forms presented for the events incorporated in the balance are preliminary proposals, and must be investigated further before a comprehensive model can be obtained. Ultimately, the model will be fitted to a wide range of industrial flotation data in order to fine tune the various balance functions and obtain an operating range for the constants in the functions. One particularly powerful outcome that is expected from the exercise is the functional dependency of coalescence frequency on frother concentration. By evaluating the frother concentration term in the coalescence frequency function for known values of frother concentration, a correlation can be derived which will allow the prediction of the coalescence rate based on frother concentration.

Once a robust population balance model is obtained, virtually all cell operating parameters will be able to be predicted. In addition to Sauter mean bubble diameter, the equilibrium gas holdup can be determined, and the influence of cell parameters such as power input, air flow rate, cell geometry and pulp density on bubble size distribution can be readily predicted. This knowledge will enable optimization of the performance of a flotation cell and will allow accurate design and simulation of flotation circuits. It is also hoped that insight gained into the fundamentals of gas dispersion will provide the impetus for the design of more efficient flotation cells.

Nomenclature

A_B	Flotation cell bulk region cross-sectional area, [m^2]
$B(v)$	Breakage frequency of bubble with volume v, [s^{-1}]
$C_{1,2...}$	Empirical constants
c_i	Number fraction of bubbles with volume i
d	Bubble diameter, [m]
D	Impeller diameter, [m]
$D(v',v)$	Distribution function for daughter fragments from drop breakage
d_{max}	Maximum stable bubble diameter, [m]
d_s	Sauter mean bubble diameter, [m]
K	Coalescence frequency, {s^{-1}]
N	Impeller rotational speed, [rev/s]
$n_o(v, t)$	Number of new bubbles sparged with volume v
N^B	Number of bubbles of vol. v in bulk zone per unit volume, [m^{-3}]
N^B (T)	Total number of bubbles in bulk zone per unit volume, [m^{-3}]
N_d	Number of daughter fragments per breakage event
n_i	Number of bubbles of n volume class i per unit volume, [$^{-3}$]
$N^I(v,t)$	Number of bubbles of vol. v in impeller region per unit vol., [$^{-3}$]
N_{We}	Weber number = $\frac{\rho u_b^2 d}{\sigma}$
P	Mechanical power input, [W]
Q^I	Pumping rate of impeller, [m^3/s]
R(v)	Recycle frequency of bubbles with volume v, [s^{-1}]
r_b	Radius of bubble, [m].
t_{ij}	Coalescence time for bubbles in volume classes i and j, [s]
u_b^2	Mean square velocity over distance equal to d.
U(v)	Bubble rise velocity, [cm/s]
v	Volume of bubble, [m^3]
V	Volume of flotation cell, [m^3]
v'	Volume of parent bubble, [m^3]
V_i	Volume of impeller region, [m^3]
v_{mean}	Mean daughter fragment volume, [m^3]

Greek symbols

λ_{ij}	Attachment efficiency between bubbles from classes i and j,
θ_{ij}	Collision efficiency between bubbles from classes i and j, [s^{-1}]
ε	Specific energy dissipation rate, [W/m^3]
ϕ	Gas holdup
μ	Viscosity [kg/m/s]
ρ	Density, [kg/m^3]
σ	Surface tension, [N/m]
σ_v	Standard deviation of daughter fragment distribution
τ_{ij}	Contact time between bubbles from classes i and j, [s]

References

1. Ahmed, N. and Jameson, G.J. The Effect of Bubble Size on the Rate of Flotation of Fine Particles. *Int J. of Min. Proc.*, vol. 14, 1985. pp. 195–215.
2. Arbiter, N., Harris, C.C. and Yap, R.F. Hydrodynamics of Flotation Cells. *Transactions of the Society of Mining Engineers, AIME*, vol. 244, 1969. pp. 134–148.
3. Calabrese, R.V., Wang, C.Y. and Bryner, N.P. Drop breakup in turbulent stirred-tank contactors: Part III: correlation for mean size and drop size distribution. *A.I.C.H.E. Journal*, 32, 1986b.
4. Calderbank, P.H. Gas Adsorption from Bubbles. *The Chem. Engr.*, 45, CE209, 1967.
5. Chatzi, E.G. and Kiparissides, C. Dynamic Simulation of Bimodal Drop Size Distributions in Low-Coalescence Batch Dispersion Systems, *Chemical Engineering Science*, vol. 47, No. 2 1992.
6. Chen, H.T. and Middleman, S. Drop size Distribution in Agitated Liquid-Liquid Systems. *A.I.C.H.E. Journal*, vol. 13, 1967. p. 989.
7. Coulalouglou, C.A. and Tavlarides, L.L. Description of Interaction Processes in Agitated Liquid-Liquid Dispersions. *Chemical Engineering Science*, vol. 32, 1977.

8. EGYA-MENSAH, D. Gas Dispersion in Mechanical Flotation Cells. M.Sc. thesis—Department of Chemical Engineering, UCT, 1997.
9. GORAIN, B.K., FRANZIDIS, J.P. and MANLAPIG, E.V. Studies on Impeller Type, Impeller Speed and Air Flow Rate in an Industrial Flotation Cell —Part 1: Effect on Bubble Size Distribution. *Minerals Engineering*, vol. 8, No. 6, 1995a.
10. GORAIN, B.K., FRANZIDIS, J.P. and MANLAPIG, E.V. Effect of Bubble Size, Gas Holdup and Superficial Gas Velocity on Metallurgical Performance in an Industrial Flotation Cell. *JKMRC Report*, 1995d.
11. HINZE, J.O. Fundamentals of the hydrodynamic mechanism of splitting in dispersion processes. *A.I.C.H.E. Journal*, vol. 1: 1955. p. 289.
12. JAMESON, G.J. and ALLUM, P. A Survey of Bubble Sizes in Industrial Flotation Cells. Report for AMIRA Ltd, 1984.
13. KARAMANEV, D.G. Rise of Gas Bubbles in Quiescent Liquids. *A.I.C.H.E. Journal*, vol. 40, No. 3, 1994.
14. KOLMOGOROFF, A.N. The local structure of turbulence in incompressible viscous fluid for very large Reynolds numbers. *Compt Rend Acad Sci USSR*, 30:301, 1941a.
15. LEE, C.-H, ERICKSON, L.E. and GLASGOW, L.A. Dynamics of Bubble Size Distribution in Turbulent Gas Liquid Dispersions. *Chemical Engineering Communications*, 1987.
16. LEVICH, V.G. Physiochemical Hydrodynamics. Prentice Hall, Englewood Cliffs, NJ, 1962.
17. LU, W.-M., HSU, R.-C., CHIEN, W.-C. and LIN, L.-C. Measurement of Local Bubble Diameters and Analysis of Gas Dispersion in an Aerated Vessel with a Disk-Turbine Impeller. *Journal of Chemical Engineering of Japan*, vol. 26, No. 5, 1993.
18. NAGARAJ, N. and GRAY, D.J. Interfacial Area and Coalescence Frequency in Gas–Slurry Stirred Reactors. *A.I.C.H.E. Journal*, vol. 33, No. 9, 1987.
19. PARTHASARATHY, R., JAMESON, G.J. and AHMED, N. Bubble breakup in stirred vessels—Predicting the Sauter mean diameter. *Chem Eng Res Des, Trans/Chem E*. 69, (A4) pp. 295–301.
20. PRINCE, M.J. and BLANCH, H.W. Bubble Coalescence and Break-Up in Air-Sparged Bubble Columns. *A.I.C.H.E. Journal*, vol. 36, No. 10, 1990.
21. TATTERSON, G.B. Fluid Mixing and Gas Dispersion In Agitated Tanks. *McGraw-Hill*, 1991.
22, TSOURIS, C. and TAVLARIDES, L.L. Breakage and Coalescence Models for Drops in Turbulent Dispersions. *A.I.C.H.E. Journal*, vol. 40, No. 3, 1994.
23. TUCKER, J.P., DEGLON, D.A., FRANZIDIS, J.P., HARRIS, M.C. AND O'CONNOR, C.T. An evaluation of a direct method of bubble size distribution measurement in a laboratory batch flotation cell. *Minerals Engineering*, 7 (5/6) 1994. pp. 667–680.
24. WU, H. and PATTERSON, G.K. Laser-Doppler measurements of turbulent-flow parameters in a stirred mixer. *Chem. Engng. Sci*. 44, 1989.
25. YIANATOS, J.B., FINCH, J.A., DOBBY, G.S. and MANQIU XU. Bubble Size Estimation in a Bubble Swarm. *J. Coll. Inter. Sci*., 126(1), 1988c.
26. YOON, R.H. and LUTTRELL, G.H. The Effect of Bubble Size on Fine Particle Flotation. *Minerals Processing and Extractive Metallurgy Review*, vol. 5, 1989. pp. 101–122. ◆